Supplemental Document

Optics EXPRESS

Spectrally resolved point-spread-function engineering using a complex medium: supplement

ANTOINE BONIFACE,[1,*] MICKAEL MOUNAIX,[1,2] BAPTISTE BLOCHET,[1,3] HILTON B. DE AGUIAR,[1] FABIEN QUÉRÉ,[4] AND SYLVAIN GIGAN[1]

[1]*Laboratoire Kastler Brossel, ENS-Université PSL, CNRS, Sorbonne Université, Collège de France, 24 rue Lhomond, 75005 Paris, France*
[2]*School of Information Technology and Electrical Engineering, The University of Queensland, Brisbane, QLD, 4072, Australia*
[3]*Department of Electrical Engineering, California Institute of Technology, Pasadena, CA 91125, USA*
[4]*Université Paris-Saclay, CEA, CNRS, LIDYL, 91191, Gif-sur-Yvette, France*
[*]*antoine.boniface@lkb.ens.fr*

Supplement DOI: https://doi.org/10.6084/m9.figshare.14134307

Parent Article DOI: https://doi.org/10.1364/OE.403578

Spectrally-resolved point-spread-function engineering using a complex medium: Appendix

ANTOINE BONIFACE,[1,*] MICKAEL MOUNAIX,[1,2] BAPTISTE BLOCHET,[1,3] HILTON B. DE AGUIAR,[1] FABIEN QUÉRÉ,[4] AND SYLVAIN GIGAN[1]

[1] *Laboratoire Kastler Brossel, ENS-Université PSL, CNRS, Sorbonne Université, Collège de France, 24 rue Lhomond, 75005 Paris, France*
[2] *School of Information Technology and Electrical Engineering, The University of Queensland, Brisbane, QLD, 4072, Australia*
[3] *Department of Electrical Engineering, California Institute of Technology, Pasadena, California 91125, USA*
[4] *Université Paris-Saclay, CEA, CNRS, LIDYL, 91191, Gif-sur-Yvette, France*
[*] *antoine.boniface@lkb.ens.fr*

Appendix

A. Procedure to obtain MSTM^{filt}

We describe based on a detailed flow chart in Fig. 1 how MSTM^{filt} is numerically obtained from the experimental MSTM. At first, we need to measure the multi-spectral transmission matrix (step ①). This is achieved by wavefront-shaping both spatially and spectrally the phase of the pulse impinging onto the scattering medium. From a camera placed on the other facet of the medium, i.e. in transmission, we can retrieve the output field using digital holography techniques. This is repeated for a full set of modes forming an orthogonal basis (here the Hadamard basis) to characterize at best the propagation of all the spectral components of the pulse. Phase conjugation (PC) of the MSTM enables focusing the pulse at any position of the

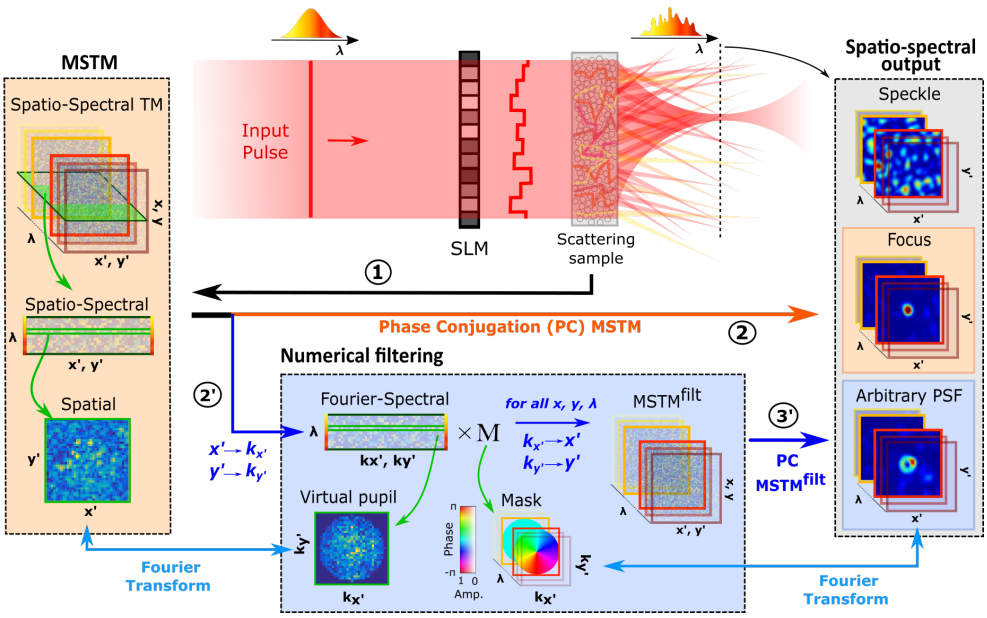

Fig. 1. General principle for spectrally-resolved PSF engineering with a scattering medium.

output plane with a controllable spectrum (step ②). To go beyond the previous approach and control the spatio-spectral PSF of the focused beam, an intermediary numerical step must be added. It consists in filtering the output field in a virtual pupil (obtained by Fourier transforming the spatial content {x', y'} of the MSTM) with a spectrally-dependent mask M hence generating $\text{MSTM}^{\text{filt}}$ (step ②'). Finally, phase conjugation of $\text{MSTM}^{\text{filt}}$ allows focusing the pulse with a spectrally-resolved PSF, defined by the Fourier transform of the arbitrary spectrally dependent mask M (step ③'). It is important to note that both MSTM and $\text{MSTM}^{\text{filt}}$ have similar dimensions: they both control the same amount of input/output modes. Also in the two cases, the phase conjugation is proceeded the same way.

B. Discussion on the effective NAs

In the following subsection, we discuss how to retrieve the NAs obtained for the different filtering presented in Fig. 4 of the manuscript and provide arguments to understand the observed experimental deviations. The effective NAs in both cases, "High NA" and "Low NA", cannot be directly determined from the diameter of the pupil. In contrast to common imaging systems, the effective NA of our optical apparatus is neither limited by the NA of the illumination nor by the collection objective, but related to the speckle grain size (as shown for instance in [1]). From the estimation of the speckle grain size, we found that in the "High NA" case the presence of the Gaussian envelope actually increases the speckle grain size by 40 % (equivalently reduces the effective NA by 40 %) compared to a uniformly distributed intensity (flat pupil). This effect is much less pronounced in the "Low NA" case, simply because on average the intensity distribution within the mask is relatively uniform. We instead estimated the effective NA from d the speckle grain size (retrieved from the speckle autocorrelation in Fig. 2.d). We obtained $NA_{HighNA} = \lambda/(2d) = 0.6$ and $NA_{LowNA} = 0.3$ for the two different masks, "High NA" and

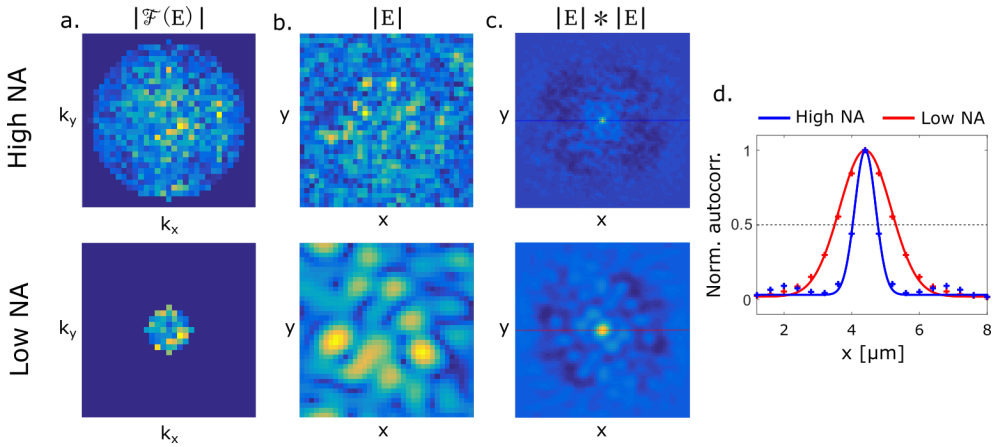

Fig. 2. Experimental data from MSTMfilt at λ = 800 nm and for a given SLM input mode (i.e. illumination) for two different numerical filtering: "High NA" (top panel) and "Low NA" (bottom panel). a. Amplitude of the electric field in k-space after filtering with masks Fig. 2.a and Fig. 2.b respectively. b. Corresponding amplitude of the speckle field in real space. c. Autocorrelation of the speckle field amplitude to estimate the speckle grain size. d. Cross section along the x-axis to extract the Full Width at Half Maximum (FWHM) with a Gaussian fit. Over 100 realizations (different field in the pupil) we obtain the autocorrelation FWHMs, $\sqrt{2}$d = 1 μm and 2 μm for "High NA" and "Low NA" respectively. It results in a ratio of $\sim$ 2 between the red and blue plots.

"Low NA" respectively. So, the ratio between these two is only a factor 2, and not a factor 3 as one would get by considering the ratio between the diameters of the applied masks.
Another important point we would like to stress here is that the estimation of both lateral and axial sizes is particularly challenging because we measure a very low intensity and noisy 2-photon signal (especially in the "Low NA" case where the PSF is broadened in all x, y and z directions). The main source of noise in our system comes from the fact that most of the output modes are not focused and contribute to the background speckle. Moreover, we divide the SLM's available degrees of freedom among the different spectral components, reducing the peak-to-background ratio of each spatio-spectral focus (see [2]). Finally, part of the light is deliberately not controlled during the numerical filtering step in k-space and contributes to the background, decreasing the peak-to-background ratio. This is particularly the case for the "Low NA" filtering. Its SNR is very low and the measurement of its lateral and axial extents is therefore not optimal.

C. Silhouette analysis

We provide in this section a statistical analysis of the experimental data of Fig. 4.e and Fig. 5.e. In these two graphs we report the lateral and axial sizes of 2-photon PSFs obtained from different filtering of the MSTM.

Although there appeared to be a rather small effect between the three generated PSFs, for each graph, we would like to prove here that our experimental data are well separated in three different clusters and the effect is statistically significant. For that, we perform a Silhouette analysis which measures how well an observation is clustered. The Silhouette value ranges from -1 to +1. Observations with a large values (close to 1) are very well clustered. If the value is around 0, it means that the observation lies between two clusters and observations with a negative

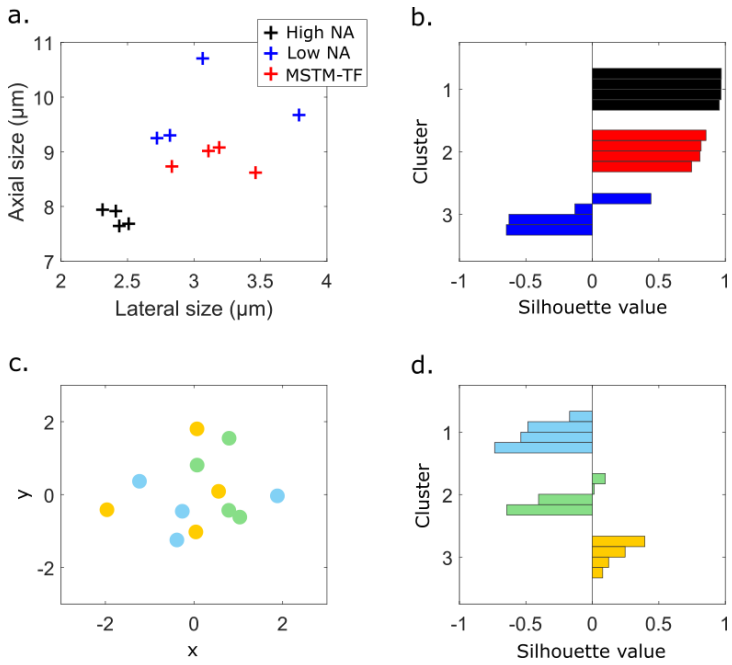

Fig. 3. (a) PSF axial size as function of lateral size (experimental data of Fig. 4.e in the manuscript). (b) Silhouette value analysis of the three clusters plotted in a. (c) Randomly positioned points in the 2D x-y plane. (d) Silhouette value analysis of the three clusters plotted in c.

Silhouette value (close to -1) are probably placed in the wrong cluster. It is usually displayed with a histogram (as in Fig. 3.b-d). In Fig. 3.b, we see that two clusters "High NA" (black bars) and "MSTM-TF" (red bars) are well defined.

The points corresponding to the "Low NA" PSF are more spread and the cluster has a larger size. This comes from the fact that in the "Low NA" case the energy is distributed over a larger area (than "High NA" for instance) because the PSF is larger and more elongated leading to a lower SNR. Lateral and axial profiles are therefore more noisy and estimations of typical sizes are less accurate. To show that this analysis is statistically significant, we compare with randomly positioned points, 3.c-d: the three clusters clearly appear and shows disparate behavior compared with the deterministic focus engineering (no Silhouette value close to 1).

We also perform a Silhouette analysis to show that an effect is also present in Fig. 5. In Fig. 4.b, we see that two clusters "High NA" (black bars) and "Bessel-TF" (red bars) are well defined. The points corresponding to the "Bessel" PSF are more spread. This comes from the fact that the "Bessel" PSF are obtained after filtering out all the low spatial frequencies in k-space leading to a lower SNR.

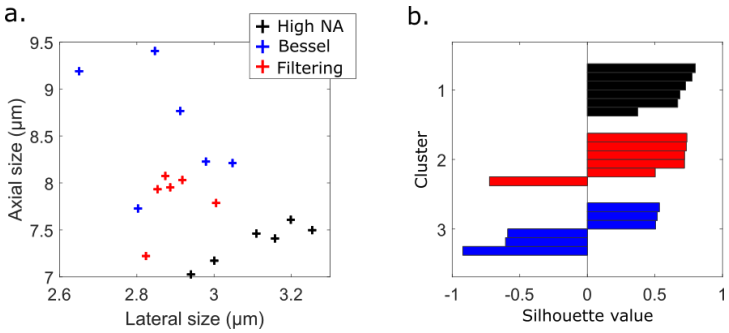

Fig. 4. (a) PSF axial size as function of lateral size (experimental data of Fig. 5.e in the manuscript). (b) Silhouette value analysis of the three clusters plotted in a.

D. Complementary simulations

In Fig. 5 we demonstrate the versatility of our technique through another spatio-spectral PSF. As in Fig. 4, the idea is to decouple the transverse spot size from the longitudinal extent, inherent to any diffraction limited optical systems. In Fig. 5, we spectrally combine "High NA" PSF with the "Bessel" one. A Bessel beam maintains tight focus (its central lobe is sub-diffraction limited) over long distances (diffraction-free propagation). The former property is interesting to improve resolution in imaging, but this comes at the cost of the sectioning. By combining a Bessel with a Gaussian beam we want to improve the lateral resolution of the Gaussian beam while maintaining a short Rayleigh length. We verified this with numerical simulations reported on in Fig. 5. In this free space analysis, we use the same masks as the one represented in Fig. 5.a of the manuscript with the parameters used experimentally but without the effect of scattering.

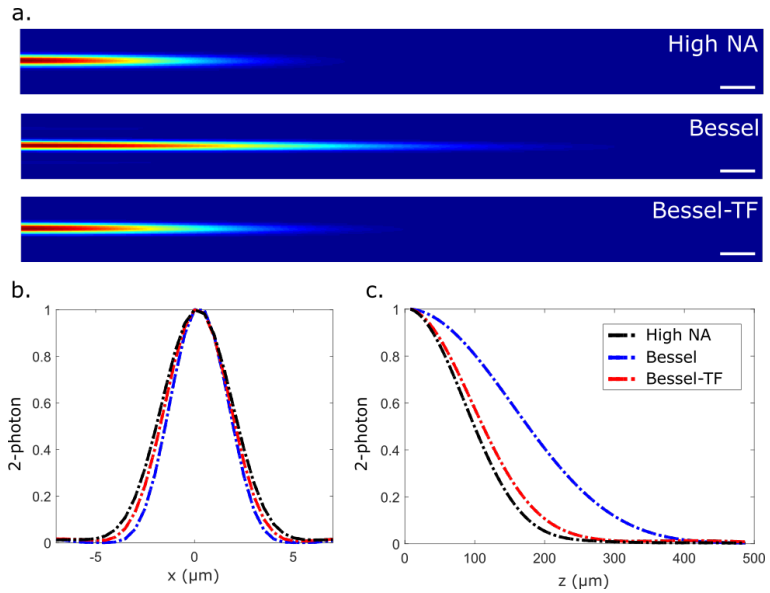

Fig. 5. Expected PSFs in free space from the masks in Fig. 5 of the manuscript – numerical simulations –. (a) Beam profiles for the three different masks. Scalebar 50 μm (b) Lateral extensions. (c) Longitudinal extension.

References

1. I. M. Vellekoop, A. Lagendijk, and A. Mosk, "Exploiting disorder for perfect focusing," Nat. photonics **4**, 320 (2010).
2. M. Mounaix, D. Andreoli, H. Defienne, G. Volpe, O. Katz, S. Grésillon, and S. Gigan, "Spatiotemporal coherent control of light through a multiple scattering medium with the multispectral transmission matrix," Phys. Rev. Lett. **116**, 253901 (2016).